Geomechanics and Engineering, *Vol. 25, No. 6 (2021) 495-508*
DOI: https://doi.org/10.12989/gae.2021.25.6.495

Risk assessment of water inrush in karst shallow tunnel with stable surface water supply: Case study

Zengguang Xu*[1], Meiting Xian[1,4c], Xiaofeng Li[2b], Wei Zhou[3b], Jiaming Wang[2b], Yaping Wang[1b] and Junrui Chai[1a]

[1]*State Key Laboratory of Eco-hydraulics in Northwest Arid Region of China, Xi'an University of Technology, Xi'an 710048, Shaanxi, China*
[2]*Hanjiang-to-Weihe River Valley Water Diversion Project Construction Co., Ltd., Xi'an 710010, Shaanxi, China*
[3]*Shaanxi Province Institute of Resources and Electric Power Investigation and Design, Xi'an 710001, Shaanxi, China*
[4]*Sichuan Water Resources and Hydroelectric Investigation & Design Institute Co. Ltd., Chengdu 610072, Sichuan, China*

(Received May 25, 2020, Revised May 26, 2021, Accepted June 13, 2021)

Abstract. Water inrush generally has a serious impact on karst shallow tunnel construction. Because of in situ fault fracture zone, high degree of weathering and poor quality of rock mass,. karst shallow tunnel would therefore face high risk of water inrush from surface during the disturbance of construction. In addition, the greater the surface water flow would contribute higher probability of water inrush under the same disaster-causing environment. However, existing research has paid less attention to the influence of surface water flow on faults or fissures water inrush. In this study, a risk assessment system of water inrush in karst shallow tunnel with stable surface water supply was firstly proposed on basis of Qinling Water Conveyance Tunnel and the Yuelongmen Tunnel in China. Each indicator was quantified and classified into four risk levels by the attribute mathematics theory and analytic hierarchy process, the degree of confidence criterion was then applied to identify the risk level of the water inrush. The evaluation results were finally verified by actual scenario on site to confirm the validity of this risk assessment system in karst shallow tunnel with stable surface water supply. Accordingly, the proposed method could be popularized and applied in future tunnel projects, because it could provide safe construction reference for karst shallow overburden tunnel with stable surface water supply.

Keywords: risk assessment; water inrush; karst shallow tunnel; stable surface water supply; attribute recognition model

1. Introduction

The number of tunnel projects is increasing because of the continuous improvement of infrastructure construction. while tunnels built in karst areas could frequently occur water inrush disasters. Shallow tunnels are generally affected by numerous factors, such as karsts, underground water, and shallow buried geological structures.

The geological disasters of a shallow karst tunnel with stable surface water supply have the characteristics of abrupt strength, rapid disaster evolution, and large range, which can lead to serious casualties and economic losses. There have been hundreds of water inrush accidents in China, each of which caused huge casualties and deterioration of engineering conditions. If the risk grade of water inrush can be predicted precisely, a series of preventive measures can be taken in advance.

In recent years, scholars at home and abroad have been doing a large number of studies on tunnels. A knotty problem in tunnel construction is that high pressure water intrudes into the tunnel (Apaydin *et al*. 2019, Alp and Apaydin 2019, Hashemnejad *et al*. 2020, Li *et al*. 2020), especially the water-rich fault. In order to safely cross the fault zone, a comprehensive evaluation method have be used to estimate the risk level of water inrush (Zhu *et al*. 2018), and then the numerical method can be used to simulate fault mechanized tunneling and TBM movement (Abdollahi *et al*. 2019). In subsea tunnels, Xue *et al*. (2019) established a cloud model considering combination weight, which can effectively predict the occurrence probability of water inrush.

The contact between soluble rock and water would accelerate the dissolution of rock, and then form a karst cave, karst cavity or solution gap contact zone, which increase the risk of water inrush (Kaufmann and Romanov 2020, Caselle *et al*. 2020, De la Torre *et al*. 2020). The factors of water inrush have been analyzed from engineering geology, hydrogeology and climate (Jing *et al*. 2017, Xu *et al*. 2019, Yuan *et al*. 2016). Based on different mathematical methods (efficacy coefficient method, AHP, attribute recognition method, set pair analysis method, cloud model), different evaluation systems of water inrush in the karst tunnel were established, and the feasibility of those methods were then verified by engineering cases (Yin *et al*. 2017, Chu *et al*. 2017, Li *et al*. 2019, Li and Yang 2018, Li and Li 2014). With the improvement of the

*Corresponding author, Professor, Ph.D.
E-mail: xuzengguang@xaut.edu.cn
[a]Ph.D.
E-mail: jrchai@xaut.edu.cn
[b]M.Eng.
[c]M.Eng. Student
E-mail: xmt183321@163.com

ISSN: 2005-307X (Print), 2092-6219 (Online)

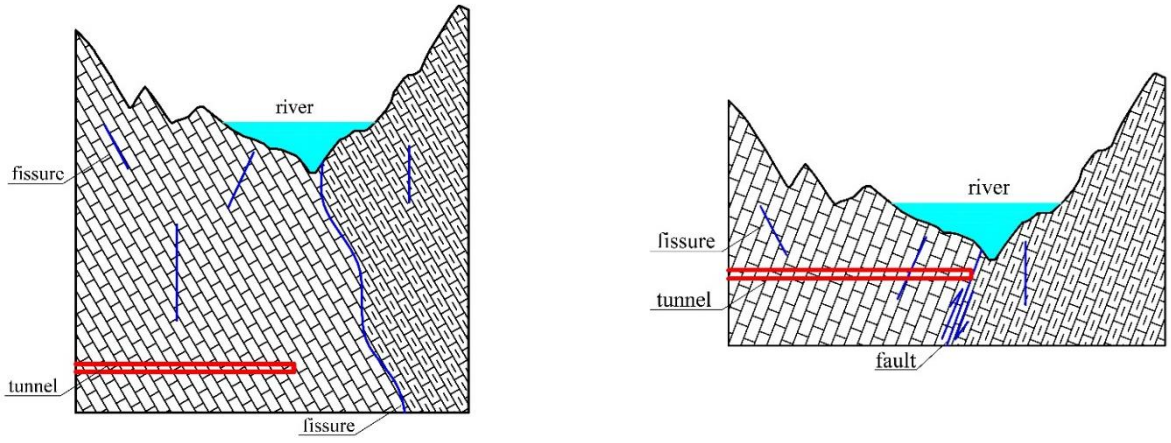

(a) Deep buried tunnel under river (b) Shallow buried tunnel under river

Fig. 1 Diagram of karst tunnel under-crossing river

evaluation method, a series of different software systems of risk assessment are gradually developed with high efficiency and accuracy of evaluation (Li *et al*. 2015, Lin *et al*. 2020). It is worth mentioning that Yau *et al*. (2020) presented a probabilistic method to predict the distribution of karst caves, which can estimate the danger of karst water intrusion into tunnels.

When a karst shallow tunnel crossing under rivers, lakes, seas or reservoirs during the disturbance of the construction, the overlying surface water would present a hydraulic relation with tunnel through the geology, such as a fault dissolution gap and karst cave, underground river. Therefore, it is a quite challenge to construct karst shallow tunnels. In the available research, however, the influence of overlying surface water flow at the fissure or fault on construction is rarely analyzed. Because of the complex geological structure, The groundwater system formed by a karst is closely connected with the surface water system, whose influence on the stability of a tunnel is more significant than that of the groundwater. When the water is abundant, it would cause a water inrush accident in the tunnel. The greater the surface water flow above the unfavorable geological zone is, the more water will flow into the tunnel, and the more serious the water inrush disaster is. Therefore, surface water flow is a particularly important disaster-causing factor, especially in shallow overburden tunnels. In this paper, a new risk assessment system of water inrush in a karst shallow tunnel with stable surface water supply is established, and applied to the Qinling Water Conveyance Tunnel under-crossing the Jiaoxi River and the Yuelongmen Tunnel under-crossing the Gaochuan River.

2. Risk assessment index system of water inrush

There are many factors affecting water inrush in karst tunnels. Sufficient water source is the prerequisite for water inrush. Fault zone, lithologic contact zone and joint fissure development zone provide migration channels for water inrush. In addition, rock weathering degree, tunnel location and excavation method also largely determine the safety of tunnel construction. The degree of disaster caused by each factor is different, and in the actual project, various factors will interact with each other. According to the research on water inrush (Li *et al*. 2013, Zhou *et al*. 2013, Peng *et al*. 2020, Xu *et al*. 2018), it can be seen that formation lithology, strata inclination, lithology contact zone, fault, surface catchment area will lead to water inrush during tunnel construction in karst area.

According to the “code for geological investigation of water conservancy and hydropower engineering”, it is stipulated in the railway water conservancy that the buried depth is greater than 300 m as a deep tunnel, and less than 300 m is a shallow tunnel. There are significant differences in rock mechanics and hydraulic characteristics between deep tunnel and shallow tunnel. When a deep tunnel under-crossing a river (as shown in Fig. 1(a)), due to the large buried depth of the tunnel and the poor connectivity of the connecting channel, the impact of surface water source on the water inrush is small, and the head pressure on the vault is mainly from the groundwater level or other water bearing structures. When a shallow tunnel is constructed under a river (as shown in Fig. 1(b)), due to the shallow buried depth of the tunnel, the influence of the groundwater level can be ignored, At this time, the surface water source is very close to the tunnel arch, under the construction disturbance, the surface water is a very dangerous disaster-causing factor, The shallower the tunnel is buried, the greater the surface water flow at the crack, and the higher the possibility of surface river invading the tunnel. Therefore, in the risk analysis of water inrush of karst shallow tunnel under river, surface water flow, tunnel buried depth and construction interference are also important disaster causing factors.

Combined with the characteristics of shallow tunnel under river, this paper analyzes from four aspects of engineering geology, geological structure, hydrogeology and tunnel characteristics, and comprehensively selects 11 main influencing factors: formation lithology, modified strata inclination, karst and non-karst contact zone, fault zone width, fault property, fissure development degree, surface water flow, surface catchment area, buried depth of tunnel, construction disturbance degree. A risk assessment

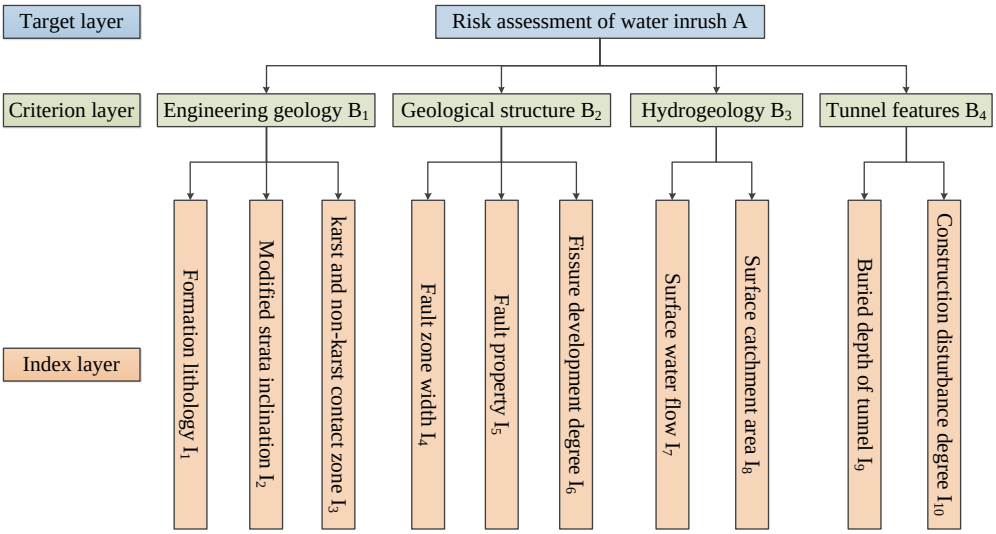

Fig. 2 Risk assessment index system of water inrush in karst shallow tunnel with stable surface water supply

Table 1 Water inrush evaluation indexes and grading standards

Evaluation index	IV(Little)	Ⅲ(Little)	Ⅱ(Medium)	Ⅰ(High)
Formation lithology (I_1)	Insoluble	Weakly soluble	Moderately soluble	Strongly soluble
Score	0~0.042	0.042~0.104	0.104~0.254	>0.254
Modified strata inclination (I_2)/°	0~5	5~10	10~25	25~45
Karst and non-karst contact zone (I_3)	None , micro	Weak	Medium	Strong
Score	100~85	85~70	70~60	60~0
Fault zone width (I_4)/m	0~1	1~5	5~10	>10
Fault property (I_5)	Compression	Torsion	Tension–torsion	Tension
Score	100~85	85~70	70~60	60~0
Fissure development degree (I_6)	None , Micro	Weak	Medium	Strong
Score	100~85	85~70	70~60	60~0
Surface water flow (I_7)/10^4 m^3/d	0~1	1~5	5~10	>10
Surface catchment area (I_8)/km^2	<5	5~7.5	7.5~10	>10
Buried depth of tunnel (I_9)/m^2	100~60	60~40	40~20	20~0
Construction disturbance degree (I_{10})	None , Micro	Weak	Medium	Strong
Score	100~85	85~70	70~60	60~0

system of water inrush in karst shallow tunnel with stable surface water supply is established as shown in Fig. 2. According to the quantitative influencing factors, the water inrush risk level standard is formulated, the danger and harm gradually increases from level IV to level I as follows: C_4 = {IV} = {Little risk}, C_3 = {III} = {Low risk}, C_2 = {II} = {Medium risk}, C_1 = {I} = {High risk}. The evaluation indexes and corresponding classification standards are shown in Table 1.

2.1 Engineering Geology B_1

Formation lithology (I_1): When a tunnel construction passes through soluble rock formations, such as limestone and dolomite, water inrush disasters are easy to occur under sufficient external water supply and construction disturbances. Rock solubility is the material basis of karst development. The higher the purity of the stratum lithology, the larger the thickness of the single layer, the more karst is developed, and the easier it is to form large karst pipelines. Based on rock solubility, it can be classified into four levels, insoluble, weakly soluble, moderately soluble and strongly soluble. The corresponding quantitative partition can be expressed by the parameter t. (Li *et al*. 2013, Zhou *et al*. 2013).

$$t = \sum_{i=1}^{3} A_i B_i = A_1 B_1 + A_2 B_2 + A_3 B_3 = 0.636 B_1 + 0.259 B_2 + 0.105 B_3 \quad (1)$$

In the formula, 0.636, 0.259 and 0.105 represent the disaster degree of strong, moderate and weak soluble rock; and B_1, B_2 and B_3 are the corresponding proportions.

Modified strata inclination (I_2): The attitude of the rock stratum has an effect on the expansion and development of the karst area, and the horizontal rock stratum is more developed than the vertical one. The permeability of groundwater in rock strata is anisotropic, and it is far less in the vertical direction than in the horizontal direction. In this

paper, strata inclination is used to describe the attitude of rock layer. Based on the existing literatures, Li *et al*. (2017) divided the revised strata inclination into four grades: 0-5°, 5°-10°, 10°-25°, and 25°-45°.

Karst and non-karst contact zone (I_3): A soluble rock endowed in a geological environment is affected by aperture gaps, cracks and pipelines at the same time, with a large void ratio. The insoluble rock is affected by both aperture gaps and cracks, the porosity is small, and the mobility of groundwater is low. The presence of an external water supply in a contact zone will accelerate the dissolution of the soluble rock layer and karst development, and form a system of large karst caves and fractures, providing space and channels for groundwater storage, recharge, and runoff. The degree of damage caused by the soluble and insoluble rock contact zone can be divided into four categories, which are unfavorable, weak favorable, medium favorable and strong favorable to karst development.

2.2 Geological structure B_2

Bad geology (I_4、I_5): The large-scale water inrush and mud out occurring during construction are closely related to the unfavorable geological conditions. The different characteristics of bad geology have different effects on the storage and migration of groundwater. The migration channel and water storage structure of inrush water mainly consider the fault of bad geology. The fault scale and the fault property determine groundwater storage and migration. The fault zone width, I_4, is used to indicate the fault scale, and the fault property, I_5, determines the fault water conductivity (Katibeh *et al*. 2010). On the basis of the disaster intensity, the fault zone width is quantitatively divided into four grades: 0-1 m, 1-5 m, 5-10 m, >10 m. The degree of damage caused by fault properties can also be classified into four levels as follows: compressional, torsional, tensional- torsional and tensional. The tensile fault has the strongest water conductivity, while the compressive fault is the weakest.

Fissure development degree (I_6): The degree of fracture development is the primary factor affecting hydraulic conductivity. With fracture development, the integrity and strength of the rock mass are damaged and the permeability increases, which provides conditions for the occurrence and migration of the groundwater. The better the fissure develops, the stronger the groundwater activity is. The possibility of water inrush accident is relatively high when tunnel construction passes through the stratum with developed rock fissure. The fracture development of rock mass is qualitatively divided into four grades, which are undeveloped or micro-developed, weakly developed, moderately developed and strongly developed.

2.3 Hydrogeology B_3

Surface water flow (I_7): The construction of shallow buried tunnels under-crossing river has attracted extensive attention of scholars at home and abroad. From the existing research, It can be seen that there is a direct relationship between surface water flow and water inrush at faults and joints (Guo *et al*. 2018). When a shallow tunnel traverses a fault zone or a fracture zone, the greater the surface water flow is, the greater the possibility of water inrush under construction disturbance is. According to the contribution degree of surface water supply flow to water inrush, it can be divided into four grades: 0-1 (10^4 m^3/d), 1-5 (10^4 m^3/d), 5-10 (10^4 m^3/d), >10 (10^4 m^3/d).

Surface catchment area (I_8): Sufficient water source is the premise of water inrush. When the surface water system above the tunnel is developed, the groundwater can be recharged through faults, joints and fissures. The richer the surface water is, the higher the probability of water inrush is. Therefore, the surface catchment area can be considered as one of the indicators to evaluate the risk level of water inrush. According to references (Li *et al*. 2013, Zhou *et al*. 2013), the surface catchment area is quantitatively divided into four levels : <5 km^2, 5-7.5 km^2, 7.5-10 km^2, >10 km^2.

2.4 Tunnel features B_4

Buried depth of tunnel (I_9): During the construction of a shallow tunnel under river, the buried depth is an important hazard factor. The shallower the buried depth is, the weaker the natural arch of surrounding rock and its own stability will be. Therefore, the excavation will further affect the shallow surface. In other words, the closer the tunnel vault is to the surface water source, the higher the possibility of surface water intruding into the tunnel. According to the disaster degree of shallow overburden tunnel depth (Yang *et al*. 2016), it can be divided into four grades: 60 ~ 100 m, 40 ~ 60 m, 20 ~ 40 m and 0 ~ 20 m.

Construction disturbance degree (I_{10}): When the tunnel is not constructed, the stress state is balanced and the rock mass is stable. In the process of excavation, construction disturbance will lead to instability of surrounding rock or damage of aquifer, thus accelerating the formation of water inrush channel. Therefore, construction disturbance degree is also considered as a disaster-causing factor for water inrush in shallow tunnels under river. According to the increasing sequence of construction disturbance to the disaster degree of water inrush disaster, the damage caused by construction disturbance can be divided into four levels: none, weak, medium and strong.

3. The attribute recognition model for assessment of water inrush

The attribute recognition model consists of two parts:

(1) Attribute mathematical theory: according to the measured value and membership function of each evaluation index, the membership degree of single index is calculated.

(2) Analytic hierarchy process: By constructing the importance judgment matrix of each evaluation index, the weight value is obtained.

Combined with the single index membership degree and weight, the comprehensive membership degree is obtained, then the risk level of water inrush is determined, and the corresponding range of water amount can be predicted. The

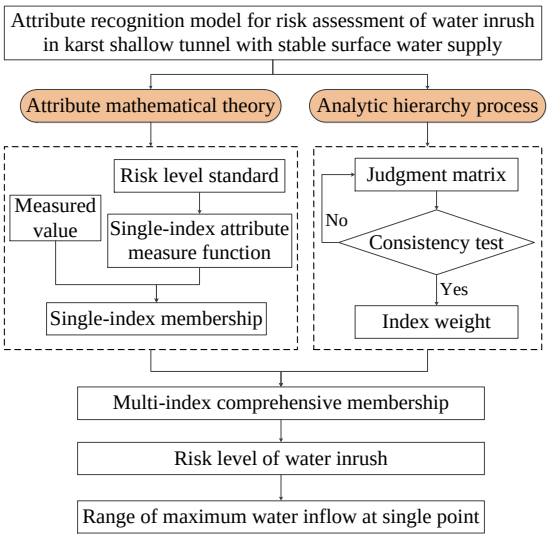

Fig. 3 Evaluation process of attribute recognition model

Table 2 Grade subdivision of the single index

Evaluation index	Evaluation grade			
	C_1	C_2	…	C_k
I_1	$a_{10} \sim a_{11}$	$a_{11} \sim a_{12}$	…	$a_{1(K-1)} \sim a_{1K}$ OR $> a_{1(K-1)}$
I_2	$a_{20} \sim a_{21}$	$a_{21} \sim a_{22}$	…	$a_{2(K-1)} \sim a_{2K}$ OR $> a_{2(K-1)}$
⋮			⋮	
I_m	$a_{m0} \sim a_{m1}$	$a_{m1} \sim a_{m2}$	…	$a_{m(K-1)} \sim a_{mK}$ OR $> a_{m(K-1)}$

basic framework of attribute recognition model is shown in Fig. 3.

3.1 Attribute mathematical theory

3.1.1 Single-index attribute measure function

When predicting and classifying the risk of water inrush in tunnels, evaluating a complex system comprehensively in engineering, the problem can be attributed to a qualitative description of the system. It is mainly used for investigating the correlation between qualitatively described metrics and different qualitative descriptions (Zhou *et al*. 2013). The magnitude of the water inrush risk with the K-level attribute C_k, is expressed by the attribute measure μ_{xk}. Therefore, the risk assessment is equivalent to evaluating the comprehensive attributes of its m index values.

In order to determine the membership grade C_k of index I_j, it is necessary to establish a single index attribute measurement function. For the attribute measure $\mu_{xjk} = \mu(x_{ij} \in C_k)(1 \le k \le K)$ of single indicator I_j under different measured value t_j, with attribute C_k. The rating subdivision of a single indicator should satisfy the form in Table 2, where a_{jk} should satisfy $a_{j0} < a_{j1} < \cdots < a_{jK}$ or $a_{j0} > a_{j1} > \cdots > a_{jK}$.

The parameters b_{jk} and d_{jk} to construct the single- index membership function are as follows:

$$b_{jk} = \frac{a_{jk-1} + a_{jk}}{2} \quad k = 1, 2, \cdots, K \tag{2}$$

$$d_{jk} = \min\left\{\left|b_{jk} - a_{jk}\right|, \left|b_{jk+1} - a_{jk}\right|\right\} \quad k = 1, 2, \cdots, K-1 \tag{3}$$

For the "bigger is superior" income-type indicators (I_1, I_2, I_4, I_7, I_8, I_9): the risk level of water inrush increases with the increase of the index value, that is, when $a_{j0} < a_{j1} < \cdots < a_{jK}$, the single-index attribute measurement function can be described as:

$$\mu_{xj1}(t) = \begin{cases} 1 & t < a_{j1} - d_{j1} \\ \dfrac{a_{j1} + d_{j1} - t}{2d_{j1}} & a_{j1} - d_{j1} \le t \le a_{j1} + d_{j1} \\ 0 & t > a_{j1} + d_{j1} \end{cases} \tag{4}$$

$$\mu_{xjk}(t) = \begin{cases} 0 & t < a_{jk-1} - d_{jk-1} \\ \dfrac{t - a_{jk-1} + d_{jk-1}}{2d_{jk-1}} & a_{jk-1} - d_{jk-1} \le t \le a_{jk-1} + d_{jk-1} \\ 1 & a_{jk-1} + d_{jk-1} < t < a_{jk} - d_{jk} \\ \dfrac{a_{jk} + d_{jk} - t}{2d_{jk}} & a_{jk} - d_{jk} \le t \le a_{jk} + d_{jk} \\ 0 & t > a_{jk} + d_{jk} \end{cases} \tag{5}$$

$$\mu_{xjK}(t) = \begin{cases} 0 & t < a_{jK-1} - d_{jK-1} \\ \dfrac{t - a_{jK-1} + d_{jK-1}}{2d_{jK-1}} & a_{jK-1} - d_{jK-1} \le t \le a_{jK-1} + d_{jK-1} \\ 1 & t > a_{jK-1} + d_{jK-1} \end{cases} \tag{6}$$

For the "smaller is better" cost-type indicators (I_3, I_5, I_6, I_{10}): the risk level of water inrush decreases with the increase of the index value, that is, when $a_{j0} > a_{j1} > \cdots > a_{jK}$, the single-index attribute measurement function can be described as:

$$\mu_{xj1}(t) = \begin{cases} 0 & t < a_{j1} - d_{j1} \\ \dfrac{t - a_{j1} + d_{j1}}{2d_{j1}} & a_{j1} - d_{j1} \le t \le a_{j1} + d_{j1} \\ 1 & t > a_{j1} + d_{j1} \end{cases} \tag{7}$$

$$\mu_{xjk}(t) = \begin{cases} 0 & t < a_{jk} - d_{jk} \\ \dfrac{t - a_{jk} + d_{jk}}{2d_{jk}} & a_{jk} - d_{jk} \le t \le a_{jk} + d_{jk} \\ 1 & a_{jk} + d_{jk} < t < a_{jk-1} - d_{jk-1} \\ \dfrac{a_{jk-1} + d_{jk-1} - t}{2d_{jk-1}} & a_{jk-1} - d_{jk-1} \le t \le a_{jk-1} + d_{jk-1} \\ 0 & t > a_{jk-1} + d_{jk-1} \end{cases} \tag{8}$$

$$\mu_{xjK}(t) = \begin{cases} 1 & t < a_{jK-1} - d_{jK-1} \\ \dfrac{a_{jK-1} + d_{jK-1} - t}{2d_{jK-1}} & a_{jK-1} - d_{jK-1} \le t \le a_{jK-1} + d_{jK-1} \\ 0 & t > a_{jK-1} + d_{jK-1} \end{cases} \tag{9}$$

In the formula, t is the measured value of assessment index, $k = 1, 2, \cdots, K-1$, $j = 1, 2, \cdots, m$.

3.1.2 Multi-index comprehensive attribute measurement analysis

The comprehensive membership degree of risk level,

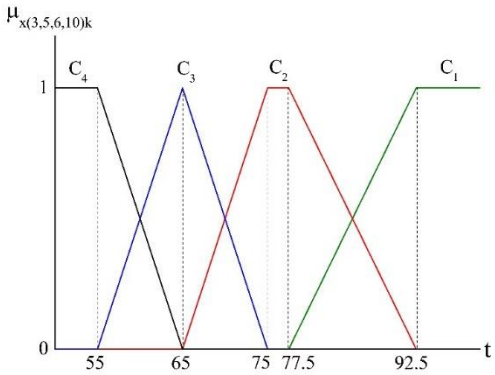

Fig. 4 The attribute measurement function of qualitative index I_3, I_5, I_6, I_{10}

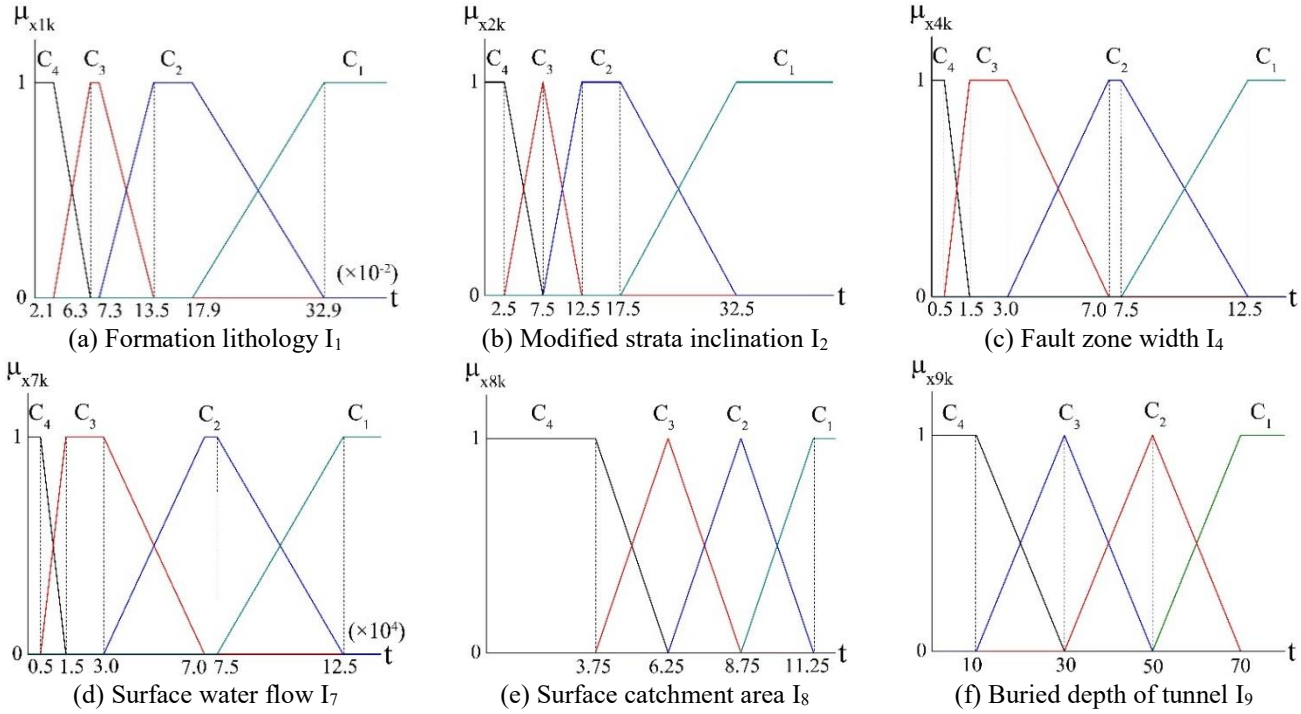

(a) Formation lithology I_1 (b) Modified strata inclination I_2 (c) Fault zone width I_4

(d) Surface water flow I_7 (e) Surface catchment area I_8 (f) Buried depth of tunnel I_9

Fig. 5 The attribute measurement function of quantitative indicators I_1, I_2, I_4, I_7, I_8, I_9.

μ_{xk}, is computed as follows:

$$\mu_{xk} = \sum_{j=1}^{m} \omega_j \mu_{xjk} \tag{10}$$

In the above formula, w_j is the weight of the jth index, which can be determined by experts and experimental data, should satisfying

$$0 \le \omega_j \le 1, \quad \sum_{j=1}^{m} \omega_j = 1 \tag{11}$$

3.1.3 Attribute recognition analysis system

For an ordered evaluation class $(C_1, C_2, \cdots, C_K)$, the confidence criterion can be used to identify which category x belongs to. λ is the confidence coefficient. In engineering applications, λ is typically between 0.6 and 0.7.

When $C_1 > C_2 > \cdots > C_K$, the risk decreases as k increases. If satisfied,

$$k_0 = \min\left\{k : \sum_{l=1}^{k} \mu_{xl} \ge \lambda,\ 1 \le k \le K\right\} \tag{12}$$

When $C_1 < C_2 < \cdots < C_K$, the risk increases as k increases. If satisfied,

$$k_0 = \max\left\{k : \sum_{l=k}^{K} \mu_{xl} \ge \lambda,\ 1 \le k \le K\right\} \tag{13}$$

Thus, x is considered to belong to the C_{k_0} level.

3.1.4 Construct attribute measure functions

According to the classification criteria in Table 1, the attribute measure function can be obtained by using Eqs. (2)-(9). The attribute measurement function of qualitative index is presented in Fig.4, and the quantitative indicators are summarized as shown in Fig.5.

3.2 Determining weight by analytic hierarchy process

AHP (Analytic Hierarchy Process) was proposed by

Table 3 Judgment matrix of the first-class indices (A-B)

A	B_1	B_2	B_3	B_4	Weight	Index
B_1	1	1	1	2	0.289	λmax=4.06
B_2	1	1	1	2	0.289	CI=0.02
B_3	1	1	1	1	0.247	RI=0.9
B_4	1	1	1	1	0.176	CR=0.023<0.10

Table 4 Judgment matrix of the second-class indices (B_1-I)

B_1	I_1	I_2	I_3	Weight	Index
I_1	1	3	1	0.416	λmax=3.01
I_2	1/3	1	1/4	0.126	CI=0.005 RI=0.58
I_3	1	4	1	0.458	CR=0.008<0.10

Table 5 Judgment matrix of the second-class indices (B_2-I)

B_2	I_4	I_5	I_6	Weight	Index
I_4	1	2	1	0.411	λmax=3.05
I_5	1/2	1	1	0.261	CI=0.03 RI=0.58
I_6	1	1	1	0.328	CR=0.046<0.10

Table 6 Judgment matrix of the second-class indices (B_3-I)

B_3	I_7	I_8	Weight	Index
I_7	1	1	0.500	λmax=2.00
I_8	1	1	0.500	CI=0.00

Table 7 Judgment matrix of the second-class indices (B_4-I)

B_4	I_9	I_{10}	Weight	Index
I_9	1	3	0.750	λmax=2.00
I_{10}	1/3	1	0.250	CI=0.00

Table 8 The weight of each layer element to target layer

Order	B_1	B_2	B_3	B_4	Weight
	0.289	0.289	0.247	0.176	
I_1	0.416	/	/	/	0.120
I_2	0.126	/	/	/	0.036
I_3	0.458	/	/	/	0.132
I_4	/	0.411	/	/	0.119
I_5	/	0.261	/	/	0.075
I_6	/	0.328	/	/	0.095
I_7	/	/	0.500	/	0.123
I_8	/	/	0.500	/	0.123
I_9	/	/	/	0.750	0.132
I_{10}	/	/	/	0.250	0.044

Saaty in the 1970s. It is a multi-criteria decision-making method that combines qualitative analysis and quantitative analysis (Saaty 1994, Wang *et al*. 2008). Based on the 1-9 scale method, the judgment matrix of each index can be obtained. The weight vector of matrix can be expressed as:

$$\overline{W_i} = n\sqrt{\prod_{j=1}^{n} a_{ij}}, \quad (i=1,2,...,n) \tag{14}$$

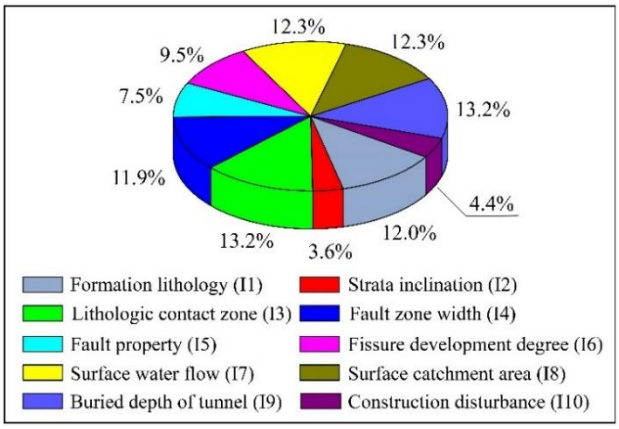

Fig. 6 Proportion of the weight values of evaluation index

Table 9 Risk grade and water quantity division of water inrush (Li *et al*. 2013)

Risk gradation	IV	III	II	I
Water inflow (m^3/d)	<500	500~3000	3000~10000	>10000

$$W = \frac{\overline{W_i}}{\sum_{j=1}^{n} \overline{W_i}}, (i=1,2,...,n) \tag{15}$$

where n is the number of evaluation indexes, $W=[W_1,W_2,...,W_n]^T$ is the eigenvector.

According to the hierarchical structure model displayed in Fig. 2, the importance comparison judgment matrix is established as shown in Tables 3-7.

In Tables 3-7, the consistency indicators meet the requirements, indicating that the distribution of weight values is reasonable. The weight calculation of each layer element to the target layer is listed in Table 8, and the proportion analysis is shown in Fig. 6.

By analyzing the weight proportion of pie chart (Fig. 6), it can be seen that surface water, fault and tunnel buried depth have great influence on water inrush risk evaluation of karst shallow tunnel under river, accounting for 24.6%, 19.4% and 13.2% of the total water inrush respectively. The modified strata inclination has the least effect on water inrush, accounting for only 3.6% of the total water inrush. Here, the surface water flow and surface catchment area are regarded as the source of water inrush disaster, and the fault, lithologic contact zone and fissure development zone are regarded as the disaster causing structures. Therefore, when the karst shallow tunnel passes through rivers, lakes, oceans or reservoirs, if there are fault fracture zone, solution gap and joint development zone in the tunnel site, the water abundance is high and the rock mass quality is poor, preventive measures must be taken in advance, to prevent surface water from invading into the tunnel.

3.3 Prediction of water inrush volume range based on risk level

According to the research of Li *et al*. (2013) and Xu *et al*. (2011) on the risk level of water inrush in karst tunnel,

the water quantity corresponding to the four grades is divided as shown in Table 9.

4. Engineering applications

4.1 The Qinling Water Conveyance Tunnel under the Jiaoxi River

4.1.1 Engineering background of the study area

The Qinling Water Conveyance Tunnel is the key project of the Hanjiang-to-Weihe River Valley Water Diversion Project, covering the Yangtze and Yellow river basins. It is the first water diversion project across the Qinling Mountains in China, and also the key project of water transfer planning of south-to-north water diversion in Shaanxi province. The tunnel is composed of Huangsan section and Yueling section, with a total length of 98.3 km, among which the Huangshan section is 16.5 km. The length of Yueling section is 81.8 km, and the maximum buried depth is 2000 m. The main geomorphologic units are the middle-low mountain area in the south of Qinling Mountains, middle-high mountainous area of the Qinling Ridge, and middle-low mountain area in the north of Qinling Mountains. Due to the complex geological conditions of the Qinling mountains, there are many knotty technical problems in construction, especially the water inrush and mud outburst.

The study area is in the K2+685~K2+962 section where the tunnel crosses Jiaoxi River under shallow overburden (as shown in Fig. 7). The Jiaoxi River basin is located in the southern slope of the Qinling mountains, is a secondary tributary of the Hanjiang river with a large amount of water. There are sanhekou–shimudi faults (f_{s2}) and yangtianba–shimudi faults (f_{s3}), forming a good water-rich area. The geological longitudinal section is shown in the Fig. 8. The buried depth of the tunnel is relatively shallow, the fault structure is crisscrossed, the joints and fissures are developed, and the surrounding rock mass is broken. Such geological conditions are conducive to the formation of water inrush channel, and under the construction disturbance, there is a high risk of water ingress from Jiaoxi River. Thus, it is difficult and risky to cross Jiaoxi River under shallow overburden. At the same time, it also has the extremely high requirements for the design and construction of the tunnel.

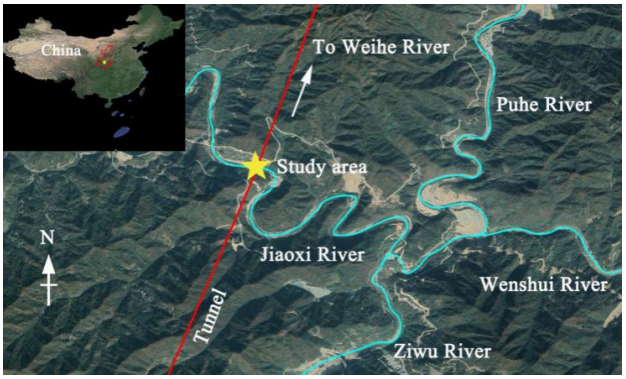

Fig. 7 Location map of study area

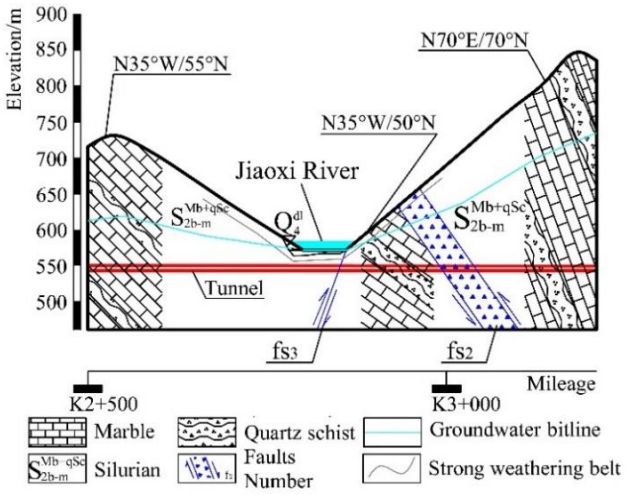

Fig. 8 Profile diagram of the tunnel under-crossing the Jiaoxi River section

4.1.2 Measurement value of evaluation index

Formation lithology I_1: The formation lithology exposed in the Jiaoxi river section is mainly middle silurian marble with quartz schist. It can be seen from the profile diagram, marble and quartz schist accounts for 80% and 20%, respectively. According to the formula, $t=\Sigma A_i B_i$, the quantitative value of the formation lithology is t=0.207.

Modified strata inclination I_2: According to the survey data and the on-site investigation of the face, the strata inclination is determined to be 55° and 50°, respectively, and the proportion is 50% in both cases. The revised rock formation inclination angles are $\varphi=25+(65-55)=35°$ and $\varphi=25+(65-50)=40°$, respectively.

Karst and non-karst contact zone I_3: In this section, there is a moderately soluble and insoluble rock contact zone between marble and quartz schist, which is moderately favorable for karst development. The score is 65 points.

Fault zone width I_4: There are two faults f_{s2} and f_{s3} in the Jiaoxi river section. The fs_2 fault is a dextral translational reverse fault, with a width of 70 meters. The f_{s3} fault is a reverse fault, with a width of 15 meters.

Fault property I_5: The results show that both the f_{s2} and fs_3 faults are reversed faults, that is, compressive faults, with an evaluation score of 90 points.

Fissure development degree I_6: As per the on-site geological survey, the rock mass of this section is relatively broken, the joint fissures and dissolution fissures are considered to be comparative development–development. Therefore, the expert score value is 60 points.

Surface water flow I_7: The river overlying the tunnel is Jiaoxi River, and the average flow of the river cross-section is measured to be 62208000 m^3/d.

Surface catchment area I_8: According to the hydrogeological conditions around the tunnel, the effective catchment area of the surface river basin is determined to be S = 20 km^2.

Buried depth of tunnel I_9: Based on the investigation data, the minimum height between the bottom of the river bed and the tunnel vault is 20 m (upper 9 m cobblestone

Table 10 Risk assessment results of water inrush of Qinling Water Conveyance Tunnel K2+685~K2+962 section

Evaluation indices	Measured value	Weight	Single index attribute measure			
			C_4	C_3	C_2	C_1
I_1	t = 0.207	0.120	0	0	0.81	0.19
I_2	55°(50%)/50°(50 %)	0.037	0	0	0	1
I_3	65	0.132	0	0	1	0
I_4	70 m / 15 m	0.119	0	0	0	1
I_5	90	0.075	0.83	0.17	0	0
I_6	60	0.095	0	0	0.50	0.50
I_7	62208000 m^3/d	0.123	0	0	0	1
I_8	S = 20 km^2	0.123	0	0	0	1
I_9	20 m	0.132	0	0	0.50	0.50
I_{10}	70	0.044	0	0.50	0.50	0
Synthetic attribute measure			0.0625	0.0348	0.3645	0.5382

layer + lower 11 m marble and quartz schist).

Construction disturbance degree I_{10}: Combined with expert evaluation, the construction interference is moderate, and the score is 70.

4.1.3 Attribute recognition analysis

In this study, the confidence coefficient λ=0.65 is used for attribute recognition. The quantitative index parameter value is substituted into the attribute measure function constructed in Fig. 4 and Fig. 5, and the single indicator membership corresponding to each risk grade is obtained. The calculated results are summarized in Table 10.

As can be seen from Table 10, when k is taken as 1, the inequality $k_0 = \max\left\{k : \sum_{l=k}^{4} \mu_{xl} \geq 0.65,\ 1 \leq k \leq 4\right\}$ is established. Specifically, the risk grade is predicted to be C_1 grade, which is high risk. According to Table 9, the predicted water volume range is greater than 10000 m^3/d.

4.1.4 Excavation verification

During the construction of the Jiaoxi river section, three large-scale water inrush accidents occurred, which are summarized in Table 11. The maximum water inflow of the three accidents was 12700 m^3 /d, 23600 m^3 /d, and 18500 m^3 /d respectively. It can be concluded that the result of the risk grade evaluation was consistent with the actual excavation. It is worth noting that a small fish was found in the tunnel during the third water inrush treatment (Li 2015, Wang 2018, Guo *et al*. 2018). It indicates that the water of Jiaoxi River intruded into the tunnel, and a leakage channel was formed between the river and the tunnel. The scene diagram of the three water inrush is shown in Fig. 9.

4.2 The Yuelongmen Tunnel under the Gaochuan River

4.2.1 Engineering background of the study area

The Yuelongmen Tunnel of Chengdu–Lanzhou Railway is constructed by dividing the work of two tunnels. The

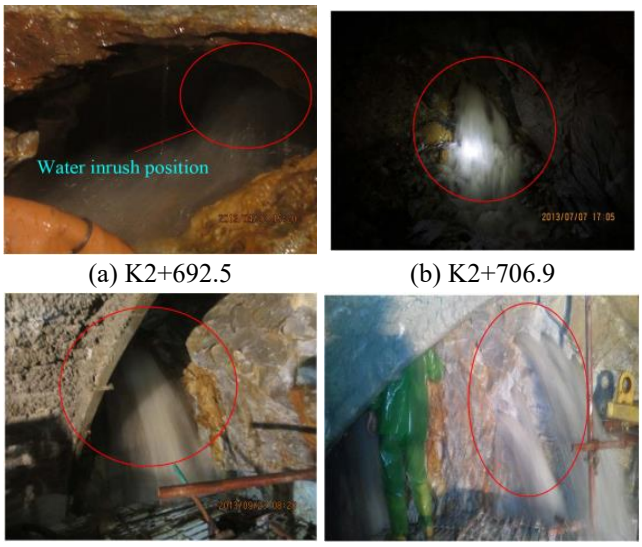

(a) K2+692.5 (b) K2+706.9

(c) Close view in K2+738 (d) Far view in K2+738

Fig. 9 Water inrush of the Qinling water conveyance tunnel crossing under Jiaoxi river (Guo *et al*. 2018)

Table 11 The actual situation of water inrush in K2+685~K2+962 sections

Water inrush	Mileage	Location	Initial water inflow（m^3/d）	Maximum water inflow（m^3/d）	Handle time (days)
First	K2+692.5	upper middle palm	1400	12700	170
Second	K2+706.9	bottom of palm face and left side wall	9800	23600	69
Third	K2+738	upper left side wall	9800	18500	13

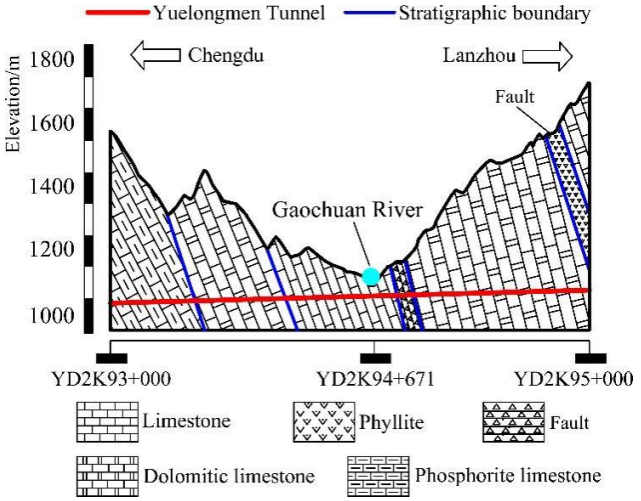

Fig. 10 Geological profile of Yuelongmen Tunnel under-crossing Gaochuan River (Xian *et al*. 2019)

lengths of the left and right line of the tunnel are 19974.3 m and 20044.0 m, respectively. The tunnel has a large buried depth, a single slope, and the maximum buried depth is 1445.5 m. The tunnel passes through a number of geological fault zones and influence zones, and the surrounding rock is weak, of which grade IV and V surrounding rock accounts for 91% of the whole line. Meanwhile, the tunnel is full of H_2S and high gas harmful

gas endangering the safety of construction personnel, so the construction risks and the construction difficulty is extremely high. It is recognized as the most difficult and rare railway project in China in the industry.

The study area is located in the shallow buried section YD2K94+621~YD2K94+701 of the tunnel under-crossing the Gaochuan river. The minimum buried depth of the tunnel is only 51 m. The engineering geology is shown in Fig. 10. There are many rivers in the mountain area of the tunnel site, and the rivers are perennial water in the valley. The tunnel construction period coincides with the rainy season, and the river has abundant water. The geological conditions are complex. The lithology of the tunnel face is mainly limestone, and the surrounding rock is grade IV. the rock mass is relatively broken, the stability is poor, and the joints and fissures are relatively developed (Xian *et al*. 2019).

Therefore, it is prone to landslides, mudslides, and water inrush. In order to ensure that the evaluation results are closer to the actual situation, this study obtains the corresponding data from expert evaluation, statistical analysis and related literature. The measured data of the project area are sorted out as follows.

4.2.2 Measurement value of evaluation index

Formation lithology I_1: According to the surrounding rock exposed on the face of the tunnel, the formation lithology is determined to be limestone with argillaceous limestone. According to the formula, $t=\Sigma A_i B_i$, the quantitative value of the formation lithology is t=0.104.

Modified strata inclination I_2: According to the survey data and the on-site investigation of the face, the strata inclination is determined to be 80°. The revised rock formation inclination angles is $\varphi=10+(80-80)=10°$.

Karst and non-karst contact zone I_3: Through expert analysis, it is determined that the contact zone of this under-crossing river section is moderately favorable for karst development, with a score of 65 points.

Fault zone width I_4: In the geological survey data, the comprehensive geophysical exploration results show that this section is obviously banded, which is inferred to be a compression fracture zone with a width of 1.5 m.

Fault property I_5: It can be seen from the above that the fault encountered in the construction area is the reverse fault, namely, the compressive property, and the score value is 90 points.

Fissure development degree I_6: According to the on-site geological survey, joint fissures and corrosion fissures are moderately developed, with a score of 70.

Surface water flow I_7: The river overlying the tunnel is Gaochuan River, and the average flow of the river cross-section is measured to be 914112 m^3/d.

Surface catchment area I_8: According to the hydrogeological conditions around the tunnel, the effective catchment area of the surface river basin is determined to be S = 12 km^2.

Buried depth of tunnel I_9: Based on the investigation data, the minimum height between the bottom of the river bed and the tunnel vault is 51 m.

Table 12 Risk assessment results of water inrush of Yuelongmen Tunnel YD2K94+621~YD2K94+701 section

Evaluation indices	Measured value	Weight	Single index attribute measure			
			C_4	C_3	C_2	C_1
I_1	t = 0.104	0.120	0	0.48	0.52	0
I_2	80°	0.037	0	0.50	0.50	0
I_3	65	0.132	0	0	1	0
I_4	1.5 m	0.119	0	1	0	0
I_5	90	0.075	0.83	0.17	0	0
I_6	70	0.095	0	0.5	0.5	0
I_7	914112 m^3/d	0.123	0	0	0	1
I_8	S = 12 km^2	0.123	0	0	0	1
I_9	51 m	0.132	0.05	0.95	0	0
I_{10}	85	0.044	0.5	0.5	0	0
Synthetic attribute measure			0.0911	0.4018	0.2601	0.2470

Fig. 11 Water inrush diagram of construction site (Xian *et al*. 2019)

Construction disturbance degree I_{10}: Combined with expert evaluation, the construction interference is weak, and the score is 85.

4.2.3 Attribute recognition analysis

In this study, the confidence coefficient λ=0.65 is used for attribute recognition. The quantitative index parameter value is substituted into the attribute measure function constructed in Fig. 4 and Fig. 5, and the single indicator membership corresponding to each risk grade is obtained. The calculated results are summarized in Table 12.

As can be seen from Table 12, when k is taken as 2, the inequality $k_0=\max\left\{k:\sum_{l=k}^{4}\mu_{xl}\geq 0.65,\ 1\leq k\leq 4\right\}$ is established. Specifically, the risk grade is predicted to be C_2 grade, which is moderately risk. According to Table 9, the predicted water volume ranges from 3000 to 10000 m^3/d.

4.2.4 Excavation verification

From the related literature (Xian *et al*. 2019), it is known that the tunnel under-crossing Gaochuan river coincides with the rainy season, the surface precipitation has a great influence on the water inrush in the tunnel. The water inflow at the tunnel face can reach 7000 m^3/d (as shown in Fig. 11), which is consistent with the predicted

Table 13 Comparison of evaluation results between attribute recognition model and other methods

Assessment samples	Assessment methodology	Membership				Hazard grade	Field actual results
		IV	III	II	I		
Qinling Water Conveyance Tunnel	Attribute recognition model	0.0625	0.0348	0.3645	0.5382	I	I
	SPA	0.0065	0.0000	0.3533	0.6402	I	I
	Fuzzy comprehensive evaluation	0.0754	0.0000	0.2557	0.6689	I	I
Yuelongmen Tunnel	Attribute recognition model	0.0911	0.4018	0.2601	0.2470	II	II
	SPA	0.0509	0.2666	0.4347	0.2477	II	II
	Fuzzy comprehensive evaluation	0.2517	0.1545	0.3468	0.2470	II	II

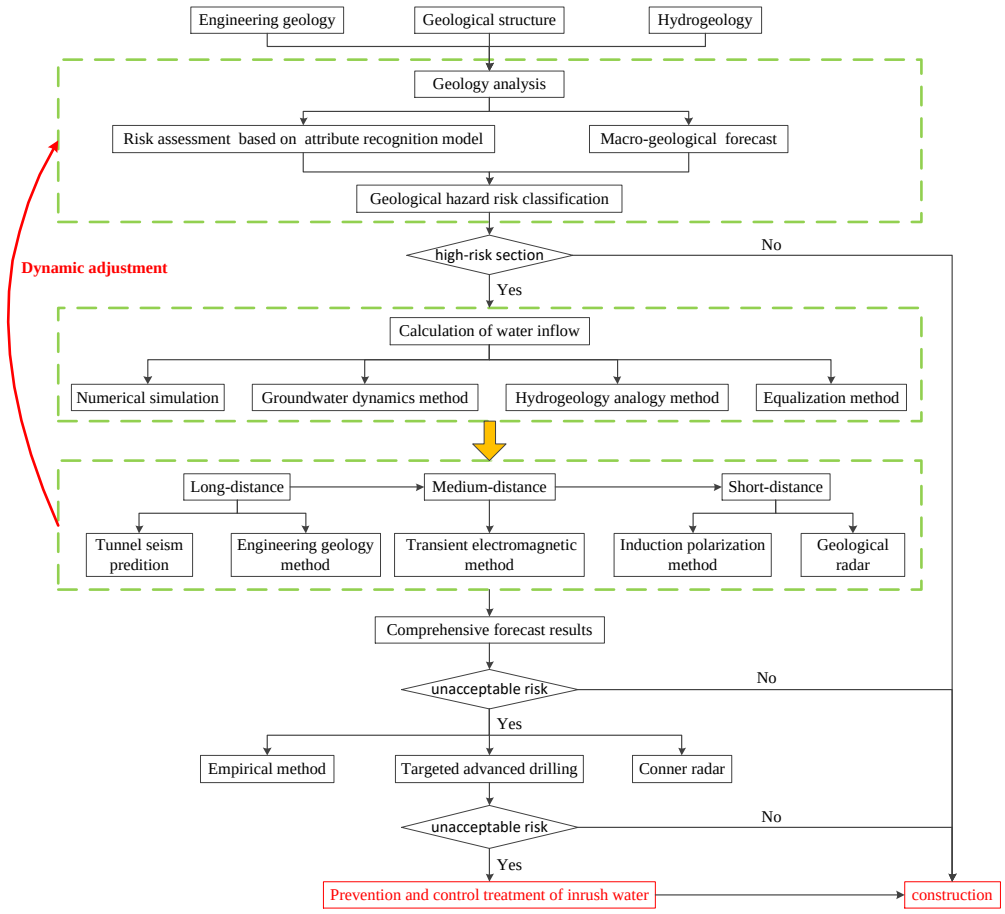

Fig. 12 Advance forecast method of the water inrush in a high-risk area of the tunnel

range of water inflow. It is proved that the proposed evaluation system and attribute recognition model for predicting water inrush in karst shallow tunnel with stable surface water supply is feasible and effective.

5. Discussion and analysis

In order to verify the rationality of the evaluation method, the evaluation results of attribute recognition model are compared with those of set pair analysis model and fuzzy comprehensive evaluation method, as shown in Table 13.

(1) Table 13 shows that the calculation results of attribute recognition model are consistent with those of SPA and fuzzy comprehensive evaluation method. Therefore, the application of attribute recognition model to the risk assessment of water inrush in tunnel. is reasonable and feasible.

(2) In the attribute recognition model, Eqs. (2)-(9) is used to determine the single index attribute measurement function, and it is unique, and the confidence criterion is used to determine the risk assessment level. However, the membership function of SPA and fuzzy comprehensive evaluation method has many forms, and the randomness is strong, the maximum membership criterion is used to judge the risk evaluation grade.

In view of the uniqueness of single index attribute measure function and the order of confidence criteria, in general, in solving the problem of multi-factor

comprehensive evaluation, the classification of attribute recognition model is more reasonable, the evaluation results are more reliable.

(3) The actual water inflow of Qinling Water Conveyance Tunnel under Jiaoxi River is much larger than that of Yuelongmen Tunnel under Gaochuan River section. From the analysis of hydrogeological conditions, compared with the shallow buried section of Gaochuan River, the stratum lithology of Jiaoxi River section is more soluble, the width of fault zone is larger, the buried depth of tunnel is shallower, and the overlaying surface river flow and catchment area are larger, so the risk level is also higher.

(4) After the risk classification of the tunnel, the low-risk area can be constructed directly. For the high-risk area, a more comprehensive risk prediction is required, and the construction can only be carried out after the corresponding preventive measures are taken. Following the statistical analysis of numerous literatures (Shi *et al*. 2017, Esmailzadeh 2018, Li *et al*. 2010), this study proposes a comprehensive risk prediction model for water inrush disasters based on risk assessment classification (as shown in Fig. 12).

Using the geological survey data and hydrogeological data of the tunnel site area, the tunnel is divided into sections according to the distribution of the stratum lithology and bad geology or the groundwater runoff modulus. Firstly, according to the attribute recognition model and the macroscopic geological forecast, the hazard levels of each section are classified. If the section is judged to be safe, construction can proceed. For high-risk sections, it is necessary to calculate the amount of water flowing into the tunnel during excavation. The methods of calculating water quantity include numerical simulation, groundwater dynamics method, hydrogeology analogy method and equalization method. On the basis of risk classification and water volume calculation, this study adopts the corresponding comprehensive advanced geological forecast, and specific forecasting schemes are selected for different geological conditions to explore the source of the tunnel water inrush disaster. If the comprehensive prediction results show an unacceptable risk, further targeted advanced drilling and in-hole radar detection will be required. For the section which is still high risk, the construction can only be carried out after the corresponding prevention and control measures are taken. In the process of forecasting, using the latest geological forecast results, we can dynamically adjust and improve the risk assessment and water quantity calculation of water inrush, improve the accuracy of the forecast, and propose the corresponding prevention and control measures, to ensure smooth progress of the tunnel construction.

6. Conclusions

(1) Based on engineering geology, geological structure hydrogeology and tunnel features of the tunnel site, 10 disaster factors are selected as formation lithology, modified strata inclination, karst and non-karst contact zone, fault zone width, fault property, fissure development degree, surface water flow, surface catchment area, buried depth of tunnel and construction disturbance degree. A risk assessment system for the water inrush in a karst shallow tunnel with stable surface water supply is established.

(2) The attribute recognition model is used to evaluate the water inrush risks of the Qinling Water Conveyance Tunnel under the Jiaoxi River and the Yuelongmen Tunnel under the Gaochuan River. Through comparative analysis with the on-site construction scenarios, SPA and fuzzy comprehensive evaluation method, verifying the feasibility and rationality of the attribute recognition model to evaluate the risk of water inrush in a karst shallow tunnel with stable surface water supply, which provides an effective method for similar projects.

(3) The water inrush disaster in a karst shallow tunnel with stable surface water supply is sudden and harmful, due to complex geological conditions and a variety of disaster-causing factors. This paper only carries out preliminary static assessment of inrush water risk by above 10 disaster factors. During construction, the dynamic monitoring data of the project should be feedback in real time, and the dynamic risk level of water inrush in each stage of construction period should be accurately evaluated by attribute recognition model.

Acknowledgments

This work was supported by the Joint Foundation of Shaanxi under [Grant number 2019JLM-57].

Conflicts of interest

There are no conflicts of interest to declare.

References

Abdollahi, M.S., Najafi, M., Bafghi, A.Y. and Marji, M.F. (2019), "A 3D numerical model to determine suitable reinforcement strategies for passing TBM through a fault zone, a case study: Safaroud water transmission tunnel, Iran", *Tunn. Undergr. Sp. Tech*., **88**, 186-199. https://doi.org/10.1016/j.tust.2019.03.008.

Alp, M. and Apaydin, A. (2019), "Assessment of the factors affecting the advance rate of the Tunnel Gerede, the longest and one of the most problematic water transmission tunnels of Turkey", *Tunn. Undergr. Sp. Tech*., **89**, 157-169. https://doi.org/10.1016/j.tust.2019.04.001.

Apaydin, A., Korkmaz, N. and Ciftci, D. (2019), "Water inflow into tunnels: assessment of the Gerede water transmission tunnel (Turkey) with complex hydrogeology", *Quart. J. Eng. Geol. Hydrogeol*., **52**(3), 346-359. https://doi.org/10.1144/qjegh2017-125.

Caselle, C., Bonetto, S., Comina, C. and Stocco, S. (2020), "GPR surveys for the prevention of karst risk in underground gypsum quarries", *Tunn. Undergr. Sp. Tech*., **95**, 103137. https://doi.org/10.1016/j.tust.2019.103137.

Chu, H.D., Xu, G.L., Yasufuku, N., Yu, Z., Liu, P.L. and Wang, J.F. (2017), "Risk assessment of water inrush in karst tunnels based on two-class fuzzy comprehensive evaluation method", *Arab. J. Geosci*., **10**(7), 179. https://doi.org/10.1007/s12517-017-2957-5.

De la Torre, B., Mudarra, M. and Andreo, B. (2020), "Investigating karst aquifers in tectonically complex alpine areas coupling geological and hydrogeological methods", *J.*

Hydrol. *X*, **6**, 100047. https://doi.org/10.1016/j.hydroa.2019.100047.

Esmailzadeh, A., Mikaeil, R., Shafei, E. and Sadegheslam, G. (2018), "Prediction of rock mass rating using TSP method and statistical analysis in Semnan Rooziyeh spring conveyance tunnel", *Tunn*. *Undergr*. *Sp*. *Tech*., **79**, 224-230. https://doi.org/10.1016/j.tust.2018.05.001.

Guo, X., Chai, J.R., Qin, Y., Xu, Z.G., Fan, Y.N. and Zhang, X.W. (2018), "Mechanism and treatment technology of three water inrush events in the Jiaoxi River Tunnel in Shaanxi, China", *J*. *Perform*. *Constr*. *Fac*., **33**(1), 04018098. https://doi.org/10.1061/(ASCE)CF.1943-5509.0001251.

Hashemnejad, A., Aghda, S.M.F. and Talkhablou, M. (2020), "Mechanized tunnelling in hydrothermally altered grounds: The effect of hydrothermal fluids on the rock behaviour in the central Iran", *Tunn*. *Undergr*. *Sp*. *Tech*., **99**, 103340. https://doi.org/10.1016/j.tust.2020.103340.

Ismail, M.A.M., Majid, T.A., Goh, C.O, Lim, S.P. and Tan, C.G. (2019), "Geological assessment for tunnel excavation under river with shallow overburden using surface site investigation data and electrical resistivity tomography", *Measurement*, **144**, 260-274. https://doi.org/10.1016/j.measurement.2019.05.025.

Katibeh, H., Sharifzadeh, M. and Farhadian, H. (2010), "Estimation of fault zone permeability with Fuzzy-Delphi AHP (FDAHP) method", *Rock Mech*. *Civ*. *Environ*. *Eng*., **3**(55), 565-581.

Kaufmann, G. and Romanov, D. (2020), "Modelling long-term and short-term evolution of karst in vicinity of tunnels", *J*. *Hydrol*., **581**, 124282. https://doi.org/10.1016/j.jhydrol.2019.124282.

Li, L.M. (2015), "The analysis of geological conditions and water gushing in Jiaoxihe section of Qinling Tunnel", *Railway Standard Des*., **59**(10), 86-89 (in Chinese). https://doi.org/10.3969 /j.issn.1003-1995.2015.04.22.

Li, L.P., Lei, T., Li, S.C., Zhang, Q.Q., Xu, Z.H., Shi, S.S. and Zhou, Z.Q. (2015), "Risk assessment of water inrush in karst tunnels and software development", *Arab*. *J*. *Geosci*., **8**(4), 1843-1854. https://doi.org/10.1007/s12517-014-1365-3.

Li, L.P., Sun, S.Q., Wang, J., Yang, W.M., Song, S.G. and Fang, Z.D. (2020), "Experimental study of the precursor information of the water inrush in shield tunnels due to the proximity of a water-filled cave", *Int*. *J*. *Rock Mech*. *Min*. *Sci*., **130**, 104320. https://doi.org/10.1016/j.ijrmms.2020.104320.

Li, S.C., Li, S.C., Zhang, Q.S., Xue, Y.G., Liu, B., Su, M.X., Wang, Z.C. and Wang, S.G. (2010), "Predicting geological hazards during tunnel construction", *J*. *Rock Mech*. *Geotech*. *Eng*., **2**(3), 232-242. https://doi.org/10.3724/SP.J.1235.2010.00232.

Li, S.C., Zhou, Z.Q., Li, L.P., Xu, Z.H., Zhang, Q.Q. and Shi, S.S. (2013), "Risk assessment of water inrush in karst tunnels based on attribute synthetic evaluation system", *Tunn*. *Undergr*. *Sp*. *Tech*., **38**, 50-58. https://doi.org/10.1016/j.tust.2013.05.001.

Li, T.Z. and Yang, X.L. (2018), "Risk assessment model for water and mud inrush in deep and long tunnels based on normal grey cloud clustering method", *KSCE J*. *Civ*. *Eng*., **22**(5), 1991-2001. https://doi.org/10.1007/s12205-017-0553-6.

Li, X.P. and Li, Y.N. (2014), "Research on risk assessment system for water inrush in the karst tunnel construction based on GIS: case study on the diversion tunnel groups of the Jinping II Hydropower Station", *Tunn*. *Undergr*. *Sp*. *Tech*., **40**, 182-191. https://doi.org/10.1016/j.tust.2013.10.005.

Lin, C.J., Zhang, M., Zhou, Z.Q., Li, L.P., Shi, S.S., Chen, Y.X. and Dai, W.J. (2020), "A new quantitative method for risk assessment of water inrush in karst tunnels based on variable weight function and improved cloud model", *Tunn*. *Undergr*. *Sp*. *Tech*., **95**, 103136. https://doi.org/10.1016/j.tust.2019.103136.

Peng, Y.X., Wu, L., Zuo, Q.J., Chen, C.H. and Hao, Y. (2020), "Risk assessment of water inrush in tunnel through water-rich fault based on AHP-Cloud model", *Geomatics Nat*. *Hazards Risk*, **11**(1), 301-317. https://doi.org/10.1080/19475705.2020.1722760.

Saaty, T.L. (1994), "How to make a decision: The analytic hierarchy process", *Interfaces*, **24**(6), 19-43. https://doi.org/10.1287/inte.24.6.19.

Shi, S.S., Bu, L., Li, S.C., Xiong, Z.M., Xie, X.K., Li, L.P., Zhou, Z.Q., Xu, Z.H. and Ma, D. (2017), "Application of comprehensive prediction method of water inrush hazards induced by unfavourable geological body in high risk karst tunnel: A case study", *Geomatics Nat*. *Hazards Risk*, **8**(2), 1407-1423. https://doi.org/10.1080/19475705.2017.1337656.

Wang, J., Li, S.C., Li, L.P., Lin, P., Xu, Z.H. and Gao, C.L. (2017), "Attribute recognition model for risk assessment of water inrush", *B*. *Eng*. *Geol*. *Environ*., **78**(2), 1057-1071. https://doi.org/10.1007/s10064-017-1159-4.

Wang, S., Li, S.C., Li, L.P., Shi, S.S., Zhou, Z.Q., Cheng, S. and Hu, H.J. (2019), "Study on early warning method for water inrush in tunnel based on fine risk evaluation and hierarchical advance forecast", *Geosciences*, **9**(9), 392. https://doi.org/10.3390/geosciences9090392.

Wang, T., Hou, K.P., Gou, Z.S. and Zhang, C.L. (2008), "Application of analytic hierarchy process to tailings pond safety operation analysis", *Rock Soil Mech*., **29**(S1), 680-686 (in Chinese). https://doi.org/10.16285/j.rsm.2008.s1.008.

Wang, X.T., Li, S.C., Xu, Z.H., Hu, J., Pan, D.D. and Xue, Y.G. (2019), "Risk assessment of water inrush in karst tunnels excavation based on normal cloud model", *B*. *Eng*. *Geol*. *Environ*., **78**(5), 3783-3798. https://doi.org/10.1007/s10064-018-1294-6.

Wang, Y.C., Jing, H.W., Yu, L.Y., Su, H.J. and Luo, N. (2017), "Set pair analysis for risk assessment of water inrush in karst tunnels", *B*. *Eng*. *Geol*. *Environ*., **76**(3), 1199-1207. https://doi.org/10.1007/s10064-016-0918-y.

Wang, Y.C., Yin, X., Geng, F., Jing, H.W., Su, H.J. and Liu, R.C. (2017), "Risk assessment of water inrush in karst tunnels based on efficacy coefficient method", *Polish J*. *Environ*. *Stud*., **26**(4), 1765-1775. https://doi.org/10.15244/pjoes/65839.

Wang, Z.X. (2018), "Reason analysis of water gushing in Jiaoxi river section of Qinling Tunnel for Han River to Wei River Water Diversion Project", *Prospect*. *Sci*. *Technol*., (6), 13 (in Chinese).

Wu, Y.J., Chen, B., Ruan, H., Wang, Q.J. and Nie, W.X. (2016), "Stability evaluation of hillside under the transmission tower based on improved attribute recognition model", *Chin*. *J*. *Rock Mech*. *Eng*., **35**(S1), 3138-3146 (in Chinese). https://doi.org/10.13722/j.cnki.jrme.2015.0322.

Xian, G., S, S.S., Zhao, Y., Xiao, G.Z., Yu, Y., Wang, J.T. and Bu, L. (2019), "Research and application of comprehensive prevention and control method for water inrush in water enriched under-crossing river tunnel", *Hazard Control Tunn*. *Undergr*. *Eng*., **1**(2), 74-82 (in Chinese). https://doi.org/CNKI:SUN:SDZH.0.2019-02-010.

Xu, Z.G., Wang, Y.P., Xiao, Y., Li, L.M., Li, Y.L. and Li, Y.B. (2018), "Risk rating index and evaluation method for water inrush in long-deep tunnels", *China J*. *Highw*. *Transp*., **31**(10), 91-100 (in Chinese). https://doi.org/CNKI:SUN:ZGGL.0.2018-10-008.

Xu, Z.H., Li, S.C., Li, L.P., Hou, J.G., Sui, B. and Shi, S.S. (2011), "Risk assessment of water or mud inrush of karst tunnels based on analytic hierarchy process", *Rock Soil Mech*., **32**(6), 1757-1766 (in Chinese). https://doi.org/10.16285/j.rsm.2011.06.038.

Xue, Y.G., Li, Z.Q., Li, S.C., Qiu, D.H., Su, M.X., Xu, Z.H., Zhou, B.H. and Tao, Y.F. (2019), "Water inrush risk assessment for an undersea tunnel crossing a fault: An analytical model", *Mar*. *Georesour*. *Geotec*., **37**(7), 816-827.

https://doi.org/10.1080/1064119X.2018.1494230.
Yang, Z., Rong, X.L., Lu, H. and Dong, X. (2016), "Risk assessment on the tunnel collapse probability by the theory of extenics in combination with the entropy weight and matter-element model", *J. Safety Environ*., **16**(2), 15-19 (in Chinese). https://doi.org/10.13637/j.issn.1009-6094.2016.02.003.
Yau, K., Paraskevopoulou, C. and Konstantis, S. (2020), "Spatial variability of karst and effect on tunnel lining and water inflow. A probabilistic approach", *Tunn*. *Undergr*. *Sp*. *Tech*., **97**, 103248. https://doi.org/10.1016/j.tust.2019.103248.
Yuan, Y.C., Li, S.C., Zhang, Q.Q., Li, L.P., Shi, S.S. and Zhou, Z.Q. (2016), "Risk assessment of water inrush in karst tunnels based on a modified grey evaluation model: Sample as Shangjiawan Tunnel", *Geomech*. *Eng*., **11**(4), 493-513. https://doi.org/10.12989/gae.2016.11.4.493.
Zhou, Z.Q., Li, S.C., Li, L.P., Shi, S.S., Song, S.G. and Wang, K. (2013), "Attribute recognition model and its application of fatalness assessment of water inrush in karst tunnels", *Rock Soil Mech*., **34**(3), 818-826 (in Chinese). https://doi.org/10.16285/j.rsm.2013.03.024.
Zhu, B.B., Wu, L., Peng, Y.X., Zhou, W.W. and Chen, C.H. (2018), "Risk assessment of water inrush in tunnel through water-rich fault", *Geotech*. *Geol*. *Eng*., **36**(1), 317-326. https://doi.org/10.1007/s10706-017-0329-2.

CC